Resonant and nondissipative tunneling in independently contacted graphene structures

F. T. Vasko*
QK Applications, San Francisco, California 94033, USA
(Received 11 December 2012; revised manuscript received 22 January 2013; published 19 February 2013)

The tunneling processes between independently contacted graphene sheets separated by thin insulator are restricted by the momentum and energy conservation laws. Because of this, both dissipative tunneling transitions, with momentum transfer due to disorder scattering, and nondissipative regime of tunneling, which appears due to intersection of electron and hole branches of energy spectrum, must be taken into account. The tunneling current density is calculated for the graphene-boron nitride-graphene layers, which is described by the tight-binding approach, and for the predominant momentum scattering by static disorder. Dependencies of current on concentrations in top and bottom graphene layers, which are governed by the voltages applied through independent contacts and gates, are considered for the back- and double-gated structures. The current-voltage characteristics of the back-gated structure are in agreement with the recent experiment [Science **335**, 947 (2012)]. For the double-gated structures, the resonant dissipative tunneling causes a 10-fold enhancement of response which is important for transistor applications.

DOI: 10.1103/PhysRevB.87.075424 PACS number(s): 72.80.Vp, 73.40.Gk, 85.30.Mn

I. INTRODUCTION

In contrast to the tunneling processes between bulk materials,[1] the tunneling between low-dimensional systems must be assisted by scattering in order to satisfy the momentum and energy conservation laws; see the results and discussions for double quantum wells or wires in Refs. 2 or 3, respectively. When the splitting energy between 2D states (this energy Δ is determined by transverse voltages applied across structure) exceeds the collision broadening energy Γ ($\hbar/\Gamma$ is the departure time), the tunneling probability appears to be proportional Γ. In conditions of tunneling resonanse, when $\Delta \ll \Gamma$, this probability is proportional to $\hbar/\Gamma$,[4] i.e., the tunnel current depends on the scattering time in the same way as the current in metallic conductor. The breakdown of the dissipative tunneling regime is possible if the energy spectrum branches are intersected and the energy-momentum conservation laws are satisfied without scattering. For example, the intersection of the parabolic electron branches in double quantum wells takes place if the magnetic field is applied perpendicularly to the tunneling direction; see Refs. 5 and 6 for the experimental data and theory. Similar intersection between the linear branches of gapless energy spectra should take place in graphene/boron nitride/graphene (G/BN/G) heterostructure. Such a structure was reported recently[7] and the tunneling transistor, which is based on the independently contacted G-sheets connected through a few monolayer BN, was demonstrated.[8] In contrast to the semiconductor heterostructure case, the independently contacted G/BN/G structures can be easily realized with the use of the single-layer-transfer technology.[9] But a complete theoretical investigation of tunneling current in such a structure is not performed yet (some numerical results on the tunneling conductance were reported recently[10] but the current-voltage characteristics were not analyzed) and a problem is timely now.

In the paper, we calculate the tunneling current I between the independently contacted top (G_t) and bottom (G_b) graphene layers separated by BN. We analyze the dependencies of I on the sheet concentrations (Fermi energies) and on Δ, which are determined by the gate voltages applied to the contacts; see Fig. 1(a). Depending on voltages applied, one can realized either electron-electron (hole-hole) or electron-hole regimes of tunneling, as it is shown in Figs. 1(b) and 1(c), respectively. In the latter case, the cross-point $E = 0$ is located between the Fermi energies ($\varepsilon_{Ft} > 0 > \varepsilon_{Fb}$ or vice versa) and *the nondissipative regime* of tunneling takes place in addition to *the resonant dissipative tunneling* transitions. The current-voltage characteristics appears to differ for these regimes. For the back-gated structure, the results are in agreement with the experimental data.[8] For double-gated structures, the resonant dissipative tunneling regime can be realized, with a 10-fold enhancement of response.

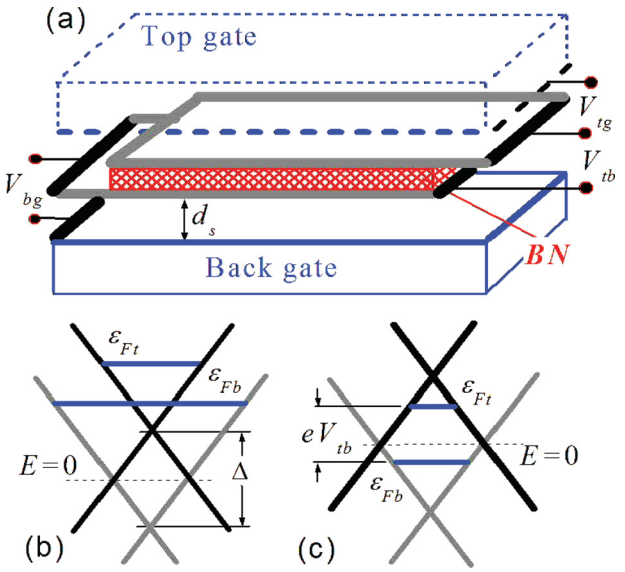

FIG. 1. (Color online) (a) G_t/BN/G_b structure under voltages V_{tb} and V_{bg} applied to top (t) and bottom (b) layers (shown by gray) through independent contacts (black); the back gate (blue) is separated by a substrate of thickness d_s and the top gate under voltage V_{tg} is shown by blue dashed lines. (b) Dispersion laws of t and b layers (black and gray crossed lines) with Fermi energies ε_{Ft} and ε_{Fb} for the electron-electron tunneling regime. (c) The same as in (b) for the electron-hole tunneling regime.

The paper is organized as follows. In Sec. II, we present the basic equations which describe the two regimes of interlayer tunneling. In Sec. III we analyze the current-voltage characteristics and compare the results for the back-gated structure with the experimental data.[8] The last section includes the discussion approximations used and the conclusions. In the Appendix, we evaluate the effective tunneling Hamiltonian for G/BN/G structure.

II. BASIC EQUATIONS

Under consideration of G_t/BN/G_b structure, we use the tunneling Hamiltonian which connects the G_t and G_b layers described by 2×2 matrices $\hat{h}_{Gt,b}$, i.e., we introduce 4×4 matrix[11]

$$\hat{H}_{\rm GBNG}=\begin{vmatrix}\hat{h}_{Gt} & \hat{\tau}\\ \hat{\tau} & \hat{h}_{Gb}\end{vmatrix}\equiv\hat{H}_G+\hat{T}. \tag{1}$$

Here we have separated the Hamiltonian of uncoupled layers, $\hat{H}_G$, and the tunneling contribution, $\hat{T}$, written through the 2×2 matrix $\hat{\tau}=\hat{\tau}^+$, which is determined by a stacking geometry of the structure; see the Appendix. The charge density in G_t and G_b layers, $Q_t^{(k)}$ (here and below $k=t,b$), and the tunnel current density, I_t, are determined through the 4×4 density matrix $\hat{\rho}_t$ by the formulas[12]

$$\begin{vmatrix}Q_t^{(k)}\\ I_t\end{vmatrix}=\frac{4}{L^2}{\rm Sp}\left(\begin{vmatrix}e\hat{P}_k\\ \hat{I}\end{vmatrix}\hat{\rho}_t\right). \tag{2}$$

Here L^2 is the normalization area, Sp(...) means both summations over states of carriers in G_t and G_b layers and averaging over lateral disorder which should be included in the Hamiltonians $\hat{h}_{Gt,b}$, and $\hat{P}_k$ is the projection operator on the k states. The interlayer current operator $\hat{I}$ is determined from the charge conservation requirement $I_t=dQ_t^{(t)}/dt=-dQ_t^{(b)}/dt$ (see similar calculations in Refs. 6), so

$$\hat{I}=\frac{e}{\hbar}\begin{vmatrix}0 & -i\hat{\tau}\\ i\hat{\tau} & 0\end{vmatrix}. \tag{3}$$

As a result, tunneling processes are described by the above-introduced matrices $\hat{T}$ and $\hat{I}$, as well as the density matrix governed by the standard equation: $i\hbar(\partial\hat{\rho}_t/\partial t)=[\hat{H}_{\rm GBNG},\hat{\rho}_t]$.[12]

Further, we separate the diagonal and nondiagonal parts of the density matrix $\hat{\rho}_t\equiv[\hat{\rho}_t]+\{\hat{\rho}_t\}$ which describe the distribution of carriers in G_t and G_b layers and the tunneling current, $I_t=(4/L^2){\rm Sp}\left(\hat{I}\{\hat{\rho}_t\}\right)$, respectively. Similarly to Ref. 6, one express $\{\rho\}$ through the carrier distributions determined by $[\rho]$ and the tunneling current density takes the form

$$I\approx\frac{4i}{L^2\hbar}\int_{-\infty}^{0}dt\,{\rm Sp}([\hat{\rho}][\hat{T},e^{-i\hat{H}_Gt/\hbar}\hat{I}e^{i\hat{H}_Gt/\hbar}]). \tag{4}$$

Calculations of Sp(...) are performed below with the use of the basis formed by two-row wave functions in kth layer $\Psi_{\mathbf{x}}^{(k\alpha)}$ determined by the eigenvalue problem $\hat{h}_{Gk}\Psi_{\mathbf{x}}^{(k\alpha)}=\varepsilon_{k\alpha}\Psi_{\mathbf{x}}^{(k\alpha)}$. We introduce the spectral density matrix, labeled by $l,l'=1$ and 2, as

$$A_{E,ll'}^{(k)}(\mathbf{x}-\mathbf{x}')=\left\langle\sum_{\alpha}\delta\left(E-\varepsilon_{k\alpha}\right)\Psi_{l\mathbf{x}}^{(k\alpha)}\Psi_{l'\mathbf{x}'}^{(k\alpha)*}\right\rangle_k, \tag{5}$$

where the averaging over random disorder in the kth layer $\langle\ldots\rangle_k$ is performed. Using the Fermi distribution for heavily doped layers, when $[\rho]$ is replaced by the θ function $\theta(\varepsilon_{Fk}-\varepsilon_{k\alpha})$ with the Fermi energies ε_{Fk} in Eq. (4), we transform I into

$$I=\frac{8\pi|e|}{\hbar L^2}\int_{\varepsilon_{Fb}}^{\varepsilon_{Ft}}dE\int d\mathbf{x}\int d\mathbf{x}'\times{\rm tr}\left[\hat{\tau}^+\hat{A}_E^{(b)}(\mathbf{x}'-\mathbf{x})\hat{\tau}\hat{A}_E^{(t)}(\mathbf{x}-\mathbf{x}')\right], \tag{6}$$

where tr(...) means summation over the matrix variable.

Below, we express $\hat{A}_E^{(k)}$ in the momentum representation as $\hat{A}_{E,\mathbf{p}}^{(k)}=i(\hat{G}_{E,\mathbf{p}}^{R(k)}-\hat{G}_{E,\mathbf{p}}^{R(k)+})/2\pi$, where $\hat{G}_{E,\mathbf{p}}^{R(k)}$ is the retarded Green's function of kth layer with the cross-point energies $\pm\Delta/2$ written through the level-splitting energy. Within the model of short-range disorder with the same statistically independent characteristics for $k=t$ and b, the Green's function in the Born approximation takes form[13]

$$\begin{aligned}\hat{G}_{E,\mathbf{p}}^{R(k)}&=\hat{P}_{\mathbf{p}}^{(+)}G_{E,p}^{(k)}+\hat{P}_{\mathbf{p}}^{(-)}G_{E,-p}^{(k)}\equiv\mathcal{G}_{Ep}^{(k)}+\frac{\hat{\boldsymbol{\sigma}}\cdot\mathbf{p}}{p}\overline{\mathcal{G}}_{Ep}^{(k)},\\ G_{E,p}^{(k)}&\approx[(E\mp\Delta/2)(1+\Lambda_{E\mp\Delta/2}+ig)-\upsilon p]^{-1},\end{aligned} \tag{7}$$

where $-\Delta/2$ and $+\Delta/2$ correspond to the t and b layers and $\upsilon\simeq 10^8$ cm/s is the carrier velocity. The projection operators on the conduction (+) and valence (−) band states, $\hat{P}_{\mathbf{p}}^{(\pm)}=[1\pm(\hat{\boldsymbol{\sigma}}\cdot\mathbf{p})/p]/2$, are written through the 2×2 isospin Pauli matrix $\hat{\boldsymbol{\sigma}}$. The self-energy contributions $(E\mp\Delta/2)(\Lambda_{E\mp\Delta/2}+ig)$ are written through the logarithmically divergent real correction which is proportional to $\Lambda_E=(g\pi)\ln(E_c/|E|)$ and the coupling constant g. This approach corresponds to the short-range scattering with the cut-off energy E_c.[14] The interlayer tunneling is described by the parameters

$$T^2={\rm tr}(\hat{\tau}^+\hat{\tau}),\quad T_s^2=\frac{1}{2}\sum_{\mu}{\rm tr}\left(\hat{\tau}^+\hat{\sigma}_\mu\hat{\tau}\hat{\sigma}_\mu\right), \tag{8}$$

which appear under the calculation of the matrix trace in Eq. (6). Using Eqs. (7) and (8) we transform the tunneling current density (6) into the form

$$I=\frac{2e}{\pi\hbar}\int_{\varepsilon_{Fb}}^{\varepsilon_{Ft}}\frac{dE}{L^2}\sum_{\mathbf{p}}(T^2{\rm Im}\mathcal{G}_{Ep}^{(t)}{\rm Im}\mathcal{G}_{Ep}^{(b)}+T_s^2{\rm Im}\overline{\mathcal{G}}_{Ep}^{(t)}{\rm Im}\overline{\mathcal{G}}_{Ep}^{(b)}), \tag{9}$$

where the explicit expressions for $\mathcal{G}_{Ep}^{(k)}$ and $\overline{\mathcal{G}}_{Ep}^{(k)}$ are determined by Eq. (7). Due to the in-plane symmetry of the problem, I is written as the double-integral over the $\mathbf{p}$ plane and the energy interval $(\varepsilon_{Ft},\varepsilon_{Fb})$.

Integrations in (9) are performed analytically for the collisionless case, $g\to 0$, and the tunneling current density is given by the sum of the dissipative current, which is $\propto\delta_\Gamma(\Delta)$, and the nondissipative contribution ($\propto\chi|\Delta|$):

$$\begin{aligned}I&\simeq J_T\begin{cases}\left(\varepsilon_{Ft}^2-\varepsilon_{Fb}^2\right)\delta_\Gamma(\Delta), & \varepsilon_{Ft}\varepsilon_{Fb}>0\\ {\rm sgn}(\varepsilon_{Ft})\left(\varepsilon_{Ft}^2+\varepsilon_{Fb}^2\right)\\ \quad\times\delta_\Gamma(\Delta)+\chi|\Delta|/2, & \varepsilon_{Ft}\varepsilon_{Fb}<0\end{cases},\\ J_T&=\frac{|e|\left(T^2+T_s^2\right)}{2\hbar^3\upsilon^2},\quad\chi=\frac{T^2-T_s^2}{T^2+T_s^2}.\end{aligned} \tag{10}$$

Here the resonant dissipative contribution (at $\varepsilon_{Ft}\varepsilon_{Fb}>0$) is written through the δ-like function $\delta_\Gamma(\Delta)=\Gamma/[\pi(\Delta^2+\Gamma^2)]$

with the phenomenological broadening $\Gamma \simeq g(\varepsilon_{Ft}+\varepsilon_{Fb})$. At $\varepsilon_{Ft}\varepsilon_{Fb}<0$, the nondissipative contribution is written through the factor χ ($0<\chi<1$ because $T^2 \geqslant T_s^2$) determined by the tunneling energies T and T_s. These parameters depend on the stacking order of the G_t/BN/G_b structure and rough estimate for the case of N-layer BN barrier[15] is determined by Eq. (A4); see the Appendix. As a result, we obtain $T, T_s \sim \gamma(\gamma/\widetilde{\varepsilon}_{\rm BN})^N$, where $\gamma \sim 0.4$ eV is the interlayer overlap integral and $\widetilde{\varepsilon}_{\rm BN} \leqslant 2.5$ eV is of the order of the c- and v-band energies in BN. We use below $T, T_s \sim 13$ μeV for $N=4$ and ~ 6 μeV for the six-layer BN barrier, which are in agreement with the experimental data of Ref. 8. The scattering parameters used in Eqs. (9) and (10) are taken from the conductivity measurements; see similar considerations in Refs. 16. We choose the cut-off energy $E_c \sim 0.2$ eV and the coupling constants $g \simeq 0.3$ or 0.15 corresponded to the maximal sheet resistance ~ 4 or 2 kΩ per square.

The current density I is dependent on ε_{Ft}, ε_{Fb}, and Δ, which are determined by the drops of voltages applied to three- or four-terminal structures; see Fig. 1(a). Before study of the current-voltage characteristics, we consider the dependencies of the total current I on these three energies. In Fig. 2 we plot the tunneling current, which is determined by Eqs. (9) and (7), versus Δ for different Fermi energies determined by $\varepsilon_F = (\varepsilon_{Ft}+\varepsilon_{Fb})/2$ and $\delta\varepsilon_F = \varepsilon_{Ft}-\varepsilon_{Fb}$ at $\chi = 1$ or 0. The resonant dissipative regime of tunneling is realized at $|\varepsilon_F| > |\delta\varepsilon_F/2|$ and peak value $I(\Delta=0)$ increases both with doping levels and with g, as shown in Fig. 2(a). If $|\varepsilon_F| < |\delta\varepsilon_F/2|$, the electron-hole tunneling regime takes place and the nondissipative contribution becomes dominant with increasing of Δ, where $I \propto \chi|\Delta|$. At small Δ the dependency $I(\Delta)$ is transformed into narrow peak due to the dissipative contribution with weak broadening; see Eq. (10) and Fig. 2(b). The numerical results given by Eq. (9) are in a good agreement with the approximations (10), shown by the dotted asymptotics, because of weak ($\leqslant 10\%$) contributions from the renormalization of energy spectra.

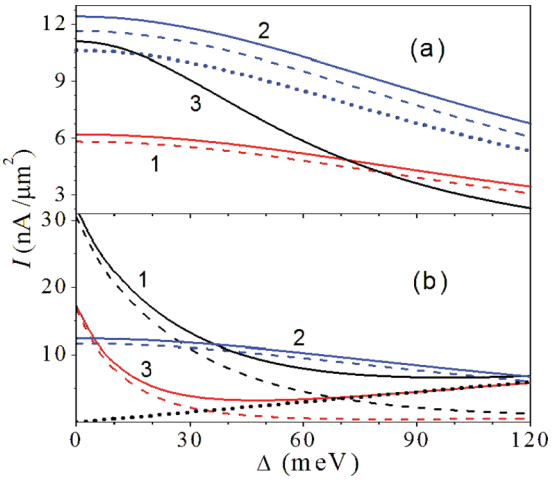

FIG. 2. (Color online) (a) Tunneling current density I versus level splitting Δ for the resonant tunneling regime at $\varepsilon_F = 200$ meV and $\delta\varepsilon = 50$ meV (1) or 100 meV (2) for $g = 0.3$. Solid and dashed curves are plotted for $\chi = 1$ and $\chi = 0$, respectively. Curve (3) is plotted for parameters (1) at $g = 0.15$. Dotted curve fits dependencies (2) with the use Eq. (10). (b) The same as in panel (a) for the nondissipative regime if $\varepsilon_F = 0$ and $\delta\varepsilon = 200$ meV (1) or 100 meV (3). Curve (2) corresponds to $\varepsilon_F = 200$ meV and $\delta\varepsilon = 100$ meV and the dotted line gives $\propto \Delta$ contribution in Eq. (10).

Neglecting the quantum capacitance contributions and the near-contact drops of potentials, we use $\varepsilon_{Ft}-\varepsilon_{Fb} \simeq eV_{tb}$ and the Gauss theorem connected the carrier concentrations in graphene with interlayer electric fields, V_{tb}/d and V_{bg}/d_s (here d and d_s are thicknesses of BN layer and SiO_2 substrate). As a result, the Fermi energies and Δ are connected with drops of voltages as follows:

$$2\varepsilon_{Ft,b} \simeq \pm eV_{tb} - F(eV_{tb}\varepsilon_d) - F(eV_{bg}\varepsilon_{d_s} - eV_{tb}\varepsilon_d),$$
$$\Delta \simeq eV_{tb} + F(eV_{tb}\varepsilon_d) - F(eV_{bg}\varepsilon_{d_s} - eV_{tb}\varepsilon_d), \quad (11)$$
$$F(x) = \mathrm{sgn}(x)\sqrt{|x|}, \quad \varepsilon_d = \frac{\epsilon(\hbar v)^2}{4e^2 d}.$$

Here "+" and "−" stand for G_t and G_b layers, $\varepsilon_{Ft,b} > 0$ or < 0 correspond to electron or hole doping, and the dielectric permittivity $\epsilon \simeq 4$ is the same for BN and SiO_2 layers; see Refs. 7 and 8. For the double-gated structure with top gate separated by BN insulator of thickness d_t, one obtains similar expressions for $\varepsilon_{Ft,b}$ and Δ after the replacement $eV_{tb}\varepsilon_d \to eV_{tb}\varepsilon_d - eV_{tg}\varepsilon_{d_t}$; see the voltages shown in Fig. 1(a). The approach (11) is valid for the heavily doped graphene layers, so the fields V_{tb}/d, V_{bg}/d_s, and V_{tg}/d_t should be strong enough. On the other hand, these fields are restricted by the breakdown condition for BN layer, when these fields should be $\ll 7$ MV/cm.[17]

III. CURRENT-VOLTAGE CHARACTERISTICS

In this section we analyze the current-voltage characteristics for the back- and double-gated structures. Below, the tunneling current density is determined by Eqs. (7) and (9) with the Fermi energies and the level splitting written through the voltages applied according to Eqs. (11). The parameters described both the elastic scattering processes and the interlayer tunnel coupling are chosen the same as for the above calculations shown in Fig. 2.

For the back-gated structure with N-layer BN barriers ($N = 4$ and 6) and $g = 0.3$ the dependencies of I versus V_{tb} at fixed V_{bg} are shown in Fig. 3 at $V_{bg} = 0$, when $I_{-V_{tb}} = -I_{V_{tb}}$.[18] The electron (hole) concentrations are $\propto V_{tb}$ and Δ is the sum of linear and square-root functions; see insets. The current-voltage characteristics $I(V_{tb})$ are in reasonable agreement with the experimental data of Ref. 8 if we used the scale factor J_T with the above-estimated T and T_s. The dependencies on χ are weak enough ($\leqslant 25\%$ for $N = 4$ and $\leqslant 10\%$ for $N = 6$, not shown). If $\Delta \sim 0$, when $V_{tb} \simeq -0.55$ V for six-layer barrier, a negative resonant contribution due to dissipative tunneling gives $\sim 30\%$ variations of the I-V characteristic. Such a peculiarity was not found in Ref. 8; it probably is due to a lateral redistributions of charges or a large-scale inhomogeneities of the samples used. The I-V characteristics of back-gated structures at $V_{bg} \neq 0$ are plotted in Fig. 4 for $N = 4$, 6 and $\chi = 1$, 0. Once again, there is a reasonable agreement of $I(V_{tb}, V_{bg})$ with the available experimental data for $N = 4$ at $V_{tb} < 0$. A visible asymmetry of I takes place if $V_{tb} \to -V_{tb}$ but deviations from experimental data increase.

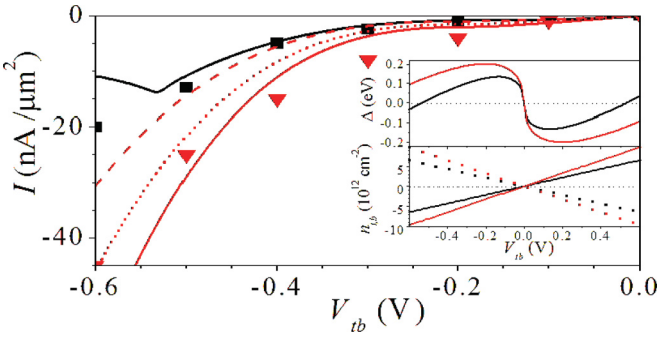

FIG. 3. (Color online) Tunneling current I versus V_{tb} at $V_{bg} = 0$ for structures with six- and four-layer BN barriers (black and red curves, respectively; squares and triangles are experimental points[8]). Solid, dotted, and dashed curves correspond to $\chi = 1.0$ 0.5, and 0. Insets show Δ and concentrations n_t or n_b (solid or dashed lines) versus V_{tb}.

The dependencies for $N = 6$ are similar but I is $\sim$2 times weaker and the resonant dissipative contribution is absent for $V_{bg} = -25$ V because $\Delta \neq 0$; see the inset.

An enhancement of the resonant dissipative tunneling contributions takes place in the double-gated (four-terminal) structure, when I depends on V_{tb}, V_{tg}, and V_{bg}. These dependencies are shown in Fig. 5 for the structure with the 10-layer BN cover layer ($d_t = 3.4$ nm; with a negligible tunneling if $d_t \gg 2$ nm[19]) at different top- and back-gate voltages ($V_{tg} = 0$ corresponds to the three-terminal structure). Since the condition $\Delta = 0$ is realized now at higher energies, the resonant dissipative tunneling peaks are >10 times greater than the background current. This is the central result which should be important for the transistor applications. Note that for $\Delta \sim 0$ at $V_{tb} \sim 0$ [curve 3 in Fig. 5(a)] the resonant dissipative peak is suppressed. Beyond this narrow region, the

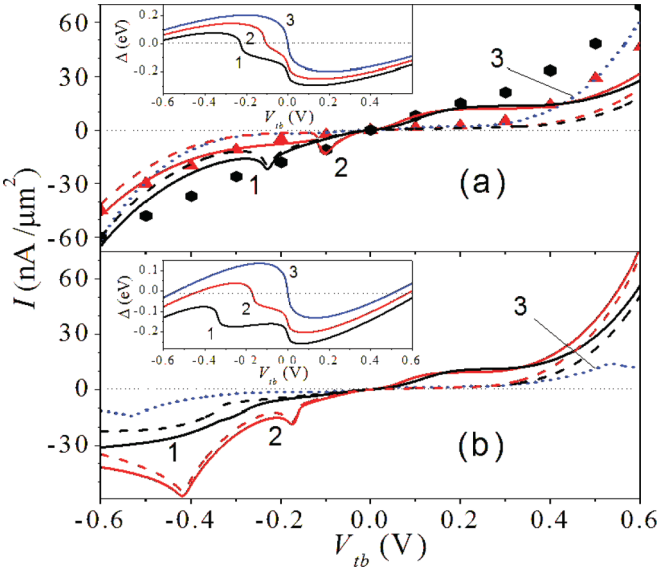

FIG. 4. (Color online) (a) Current density I versus V_{tb} for four-layer BN barrier at $V_{bg} = 0$ (red), -25 V (blue), and -50 V (black). Experimental points are shown for $V_{bg} = 0$ (triangles) and -50 V (hexagons). Inset shows Δ versus V_{tb}. (b) The same as in panel (a) for the six-layer BN barrier.

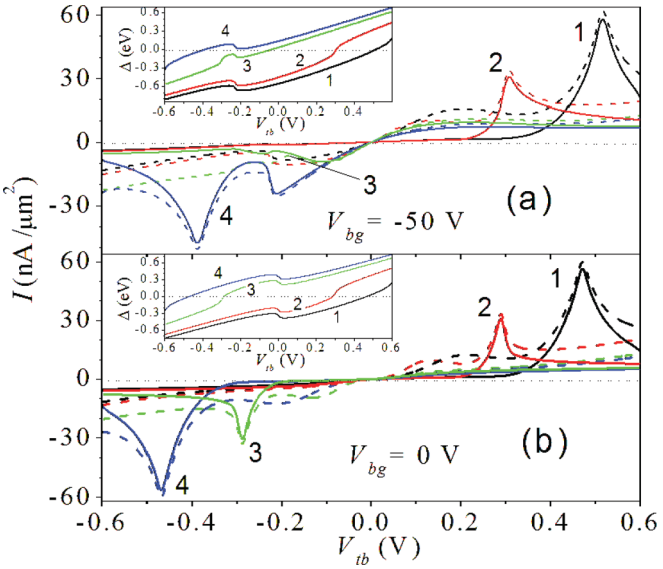

FIG. 5. (Color online) (a) Dependencies $I(V_{tb})$ for a double-gated structure with a four-layer BN barrier and a 10-layer BN cover layer under $V_{bg} = -50$ V and $V_{tg} = 1.5$ V (1), 0.75 V (2), -0.75 V (3), and -1.5 V (4). Inset shows Δ versus V_{tb}. Solid and dashed curves correspond to $\chi = 0$ and 1, respectively. (b) The same as in upper panel for $V_{bg} = 0$ V.

resonant condition $\Delta(V_{tb}) \approx 0$ should not be suppressed by lateral inhomogeneities and the peaks caused by the resonant dissipative tunneling should not be smeared.

Overall, the consideration presented here gives an adequate theoretical description of the tunneling transistor effect which is in reasonable agreement with the experimental data.[8] The analysis performed opens a way for the verification of scattering mechanisms and tunneling parameters in G/BN/G structures. In addition, the double-gated (four-terminal) structure was not considered before and this structure show a great (10 times) enhancement of tunneling current tunability.

IV. CONCLUSION

We have adopted the theory of low-dimensional tunneling[4,6] to the case of the tunneling charge transfer in independently contacted graphene structures with multilayer BN barrier taking into account the two basic mechanisms of charge transfer: resonant dissipative tunneling and nondissipative tunneling. Both the nondissipative tunneling current and the nonresonant dissipative tunneling processes are responsible for the current-voltage characteristics of back-gated structures.[8] The resonant dissipative tunneling regime is achieved for the double-gated structures and these devices demonstrate a 10-fold enhancement of I-V characteristics, which is important for transistor applications.

Further, we discuss the assumptions used. Because of a luck of data on stacking order in G/BN/G structures the tunneling energies T and T_s were estimated from the current-voltage characteristics of Ref. 8 and this result is in agreement with the tight-binding model.[15] More accurate estimates for T and T_s should be based on additional structural measurements. The simplified electrostatics description, given by Eq. (11), fails for the low-doped G_t or G_b layers, under weak interlayer

fields applied. In these narrow regions, a more complicated description, which involves the quantum capacitance effect and the contact phenomena, should be applied. The rest of the assumptions (the model of elastic scattering,[16] identical scattering in $G_{t,b}$ layers, weakness of long-range disorder, and the single-particle approach) are rather standard.

To conclude, we believe that the description of tunneling processes is an essential part of physics of graphene and the results obtained can be applied for a characterization of scattering mechanisms and tunneling parameters in the tunnel-coupled graphene structures. More importantly, these results open a way to improveme a tunneling transistor, a new type of graphene-based device. We believe that our study will stimulate a further investigation of these device applications.

APPENDIX: TUNNELING HAMILTONIAN

Below we describe the tunnel-coupled states in a G/BN/G structure using the six-column wave function $[\psi_t,\phi,\psi_b]$, which is written through the spinors $\psi_{t,b}$ corresponding to the G_t and G_b graphene layers. These layers are connected through the spinor ϕ described the single BN layer. Within the tight-binding approach,[15] the eigenstate of energy E is determined by the problem written through the 6×6 Hamiltonian,

$$\begin{vmatrix} \hat{h}_{G_t}-E & \hat{h}_{\rm GBN} & 0 \\ \hat{h}^{+}_{\rm GBN} & \hat{h}_{\rm BN}-E & \hat{h}_{\rm BNG} \\ 0 & \hat{h}^{+}_{\rm BNG} & \hat{h}_{G_b}-E \end{vmatrix} \begin{vmatrix} \psi_t \\ \phi \\ \psi_b \end{vmatrix} = 0, \qquad \text{(A1)}$$

where $\hat{h}_{G_t}$ and $\hat{h}_{G_b}$ are the 2×2 Hamiltonians of the G_t, G_b, and BN layers, while $\hat{h}_{\rm GBN}$ and $\hat{h}_{\rm BNG}$ describe weak interlayer coupling of G_t and G_b sheets with the BN layer. Under a transverse voltage applied, $\hat{h}_{G_{t,b}}=\hat{h}_G\pm\Delta/2$, where $\hat{h}_G$ is the Hamiltonian of single graphene layer and Δ is a splitting energy between the cross-points in the G_t and G_b layers. For the low-energy ($|E|<1$ eV) states, if $|E|\ll|\varepsilon_{c,v}|$, where $\varepsilon_c\sim$3.4 eV and $\varepsilon_v\sim$-1.4 eV are the c- and v-band extrema energies in BN, we can eliminate the spinor ϕ from the system (A1). As a result, the eigenstate problem is determined by the 4×4 effective tunneling Hamiltonian

$$\begin{vmatrix} \hat{h}_G+\hat{\tau}_t-E & \hat{\tau} \\ \hat{\tau}^{+} & \hat{h}_G+\hat{\tau}_b-E \end{vmatrix} \begin{vmatrix} \psi_t \\ \psi_b \end{vmatrix} = 0. \qquad \text{(A2)}$$

Here the 2×2 matrix $\hat{\tau}$ describes tunneling through BN insulator, while $\hat{\tau}_t$ and $\hat{\tau}_b$ correspond to the tunneling renormalization of t and b states:

$$\begin{aligned} &\hat{\tau}\approx-\hat{h}_{\rm GBN}\hat{h}^{-1}_{\rm BN}\hat{h}_{\rm BNG}, \\ &\hat{\tau}_t\approx-\hat{h}_{\rm GBN}\hat{h}^{-1}_{\rm BN}\hat{h}^{+}_{\rm GBN}, \quad \hat{\tau}_b\approx-\hat{h}^{+}_{\rm BNG}\hat{h}^{-1}_{\rm BN}\hat{h}_{\rm BNG}. \end{aligned} \qquad \text{(A3)}$$

Thus, we arrive to the Hamiltonian (1) with the renormalization contributions $\hat{\tau}_{t,b}$ included to $\hat{h}_{G_{t,b}}$; these corrections are negligible for the weak tunneling regime.

For the case of an N-layer BN insulator, we consider the $2(N+2)$-column wave function with N-spinors $\phi_1,\ldots,\phi_N$ described the BN layers. These states are coupled by the interlayer hopping matrices $\hat{h}_{\rm BNBN}$ and $\hat{h}^{+}_{\rm BNBN}$, which are placed at the upper and lower subdiagonals of $2(N+2)\times 2(N+2)$ Hamiltonian.[15] After eliminations of the spinors $\phi_1,\ldots,\phi_N$ from the tight-binding eigenstate problem, we arrive at Eq. (A3), where the nondiagonal matrix $\hat{\tau}$ is replaced by

$$\hat{\tau}_N\approx-\hat{h}_{\rm GBN}\left(\hat{h}^{-1}_{\rm BN}\hat{h}_{\rm BNBN}\right)^{N-1}\hat{h}^{-1}_{\rm BN}\hat{h}_{\rm BNG}. \qquad \text{(A4)}$$

For the numerical estimates of T and T_s given by Eq. (8) we assume that the diagonal matrix $\hat{h}^{-1}_{\rm BN}$ is of the order of $\widetilde{\varepsilon}^{-1}_{\rm BN}$, where $\widetilde{\varepsilon}_{\rm BN}$ is determined by $\varepsilon_{c,v}$. The hopping matrices $\hat{h}_{\rm GBN}$, $\hat{h}_{\rm BNG}$, and $\hat{h}_{\rm BNBN}$ are estimated by the interlayer overlap integral γ and they are strongly dependent on a stacking order of the G/BN/G structure.

*ftvasko@yahoo.com

[1] E. L. Wolf, *Principles of Electron Tunneling Spectroscopy* (Oxford University Press, New York, 2012).

[2] J. Smoliner, E. Gornik, and G. Weimann, Phys. Rev. B **39**, 12937 (1989); J. P. Eisenstein, Superlatt. Microstruct. **12**, 107 (1992).

[3] J. Wang, P. H. Beton, N. Mori, L. Eaves, H. Buhmann, L. Mansouri, P. C. Main, T. J. Foster, and M. Henini, Phys. Rev. Lett. **73**, 1146 (1994); N. Mori, P. H. Beton, J. Wang, and L. Eaves, Phys. Rev. B **51**, 1735 (1995).

[4] R. F. Kazarinov and R. A. Suris, Sov. Phys. Semicond. **6**, 120 (1972) [Fiz. Tekh. Poluprov. **6**, 148 (1972)].

[5] J. P. Eisenstein, T. J. Gramila, L. N. Pfeiffer, and K. W. West, Phys. Rev. B **44**, 6511 (1991); J. A. Simmons, S. K. Lyo, J. F. Klem, M. E. Sherwin, and J. R. Wendt, *ibid.* **47**, 15741 (1993).

[6] L. Zheng and A. H. MacDonald, Phys. Rev. B **47**, 10619 (1993); O. E. Raichev and F. T. Vasko, J. Phys.: Condens. Matter **8**, 1041 (1996).

[7] L. A. Ponomarenko, A. K. Geim, A. A. Zhukov, R. Jalil, S. V. Morozov, K. S. Novoselov, I. V. Grigorieva, E. H. Hill, V. V. Cheianov, V. I. Falko, K. Watanabe, T. Taniguchi, and R. V. Gorbachev, Nat. Phys. **7**, 958 (2011).

[8] L. Britnell, R. V. Gorbachev, R. Jalil, B. D. Belle, F. Schedin, M. I. Katsnelson, L. Eaves, S. V. Morozov, N. M. R. Peres, J. Leist, A. K. Geim, K. S. Novoselov, and L. A. Ponomarenko, Science **335**, 947 (2012).

[9] K. S. Novoselov, A. K. Geim, S. V. Morozov, D. Jiang, Y. Zhang, S. V. Dubonos, I. V. Grigorieva, and A. A. Firsov, Science **306**, 666 (2004).

[10] S. B. Kumar, G. Seol, and J. Guo, Appl. Phys. Lett. **101**, 033503 (2012).

[11] For general consideration of the tunneling Hamiltonian approach see Ref. 1 and monograph by F. T. Vasko and A. Kuznetsov, *Electronic States and Optical Transitions in Semiconductor Heterostructures* (Springer, New York, 1998).

[12] F. T. Vasko and O. E. Raichev, *Quantum Kinetic Theory and Applications* (Springer, New York, 2005).

[13] T. Ando, J. Phys. Soc. Jpn. **75**, 074716 (2006); T. Stauber, N. M. R. Peres, and A. H. Castro Neto, Phys. Rev. B **78**, 085418 (2008); F. T. Vasko and V. V. Mitin, *ibid.* **84**, 155445 (2011).

[14]We use the model of disorder with random potentials $V_{\mathbf{x}}$ described by the Gaussian correlator $\langle V_{\mathbf{x}} V_{\mathbf{x}'}\rangle$, with the averaged amplitude $\overline{V}$, and the correlation length l_c, if the cut-off energy $E_c \simeq \upsilon\hbar/l_c$ exceeds the energy scale under consideration. For the low-energy region, $|E| \ll E_c$, the model gives $\propto E$ relaxation rate, i.e., we deal with a short-range scattering and the coupling constant is given by $g = (\overline{V}^2 l_c/\hbar\upsilon)^2\pi/2$.

[15]J. Slawinska, I. Zasada, and Z. Klusek, Phys. Rev. B **81**, 155433 (2010); R. M. Ribeiro and N. M. R. Peres, *ibid.* **83**, 235312 (2011).

[16]F. T. Vasko and V. Ryzhii, Phys. Rev. B **76**, 233404 (2007); N. M. R. Peres, Rev. Mod. Phys. **82**, 2673 (2010).

[17]C. R. Dean, A. F. Young, I. Meric, C. Lee, L. Wang, S. Sorgenfrei, K. Watanabe, T. Taniguchi, P. Kim, K. L. Shepard, and J. Hone, Nat. Nanotechnol. **5**, 722 (2010).

[18]From Eq. (9) one obtains $I_{-\Delta} = -I_{\Delta}$, $I_{-\delta\varepsilon_F} = -I_{\delta\varepsilon_F}$, and $I_{-\varepsilon_F} = I_{\varepsilon_F}$. According to Eq. (11), Δ and $\varepsilon_{Ft,b}$ are even functions of voltages, so I remains the same under $V_{tb,bg} \to -V_{tb,bg}$ or $V_{tg,tb,bg} \to -V_{tg,tb,bg}$.

[19]F. Amet, J. R. Williams, A. G. F. Garcia, M. Yankowitz, K. Watanabe, T. Taniguchi, and D. Goldhaber-Gordon, Phys. Rev. B **85**, 073405 (2012).